Received: 18 April 2025 | Revised: 4 September 2025 | Accepted: 23 September 2025

DOI: 10.1111/aab.70065

ORIGINAL ARTICLE

Annals of Applied Biology
An international journal of the AAB

WILEY

Polarization vision and the physiological basis for trichromatic vision in *Philaenus spumarius*: Understanding host-seeking behaviour in insect vectors for *Xylella fastidiosa* control

Domen Lazar[1,2] | **Elizabeth Clark**[3] | **Andrej Meglič**[4] | **Daniele Cornara**[1] | **Gregor Belušič**[2]

[1]Department of Soil, Plant and Food Science, University of Bari, Bari, Italy

[2]Biotechnical Faculty, Department of Biology, University of Ljubljana, Ljubljana, Slovenia

[3]Advanced Light Source, Lawrence Berkeley National Laboratory, Berkeley, California, USA

[4]Eye Hospital, University Medical Centre, Ljubljana, Slovenia

Correspondence
Daniele Cornara, Department of Soil, Plant and Food Science, University of Bari, Via Amendola 165/A, 70126 Bari, Italy.
Email: daniele.cornara@uniba.it

Funding information
European Union-NextGeneration EU, National Recovery and Resilience Plan (NRRP)—mission 4 component 2 investment 1.1—'Fund for the National Research Program and for Projects of National Interest (NRP)', Grant/Award Number: CUP H53D23010620001; Italian Ministry of Agriculture, Food Sovereignty and Forestry (MASAF), Grant/Award Number: D23C22001020001; AFOSR/EOARD, Grant/Award Number: FA8655-23-1-7049; Slovenian Research Agency, Grant/Award Number: P3-0333

Abstract

In European outbreaks, the meadow spittlebug *Philaenus spumarius* is the primary vector of the xylem-limited bacterium *Xylella fastidiosa*. The mechanisms underlying host plant location by spittlebugs—critical for the transmission of associated bacterial pathogens—remain poorly understood, particularly with respect to the potential role of visual cues. Here, we investigated the visual system of *P. spumarius* through an integrated anatomical, optical, physiological, and behavioural approach to explore the potential role of vision in host-seeking behaviour. Using microscopy, 3D reconstructions, and single-cell recordings, we examined the structure and function of the compound eyes. Optical mapping revealed relatively low spatial resolution, with interommatidial angles of 4°–8° and somewhat smaller angles and finer visual sampling in central and anterior-ventral regions. Intracellular recordings showed that photoreceptors are maximally sensitive to ultraviolet (UV), blue (B), and green (G) light, suggesting the potential for trichromatic colour vision. UV and B-sensitive photoreceptors exhibited high polarization sensitivity (PS), with UV and B photoreceptors maximally sensitive to vertically and horizontally or obliquely polarized light, respectively. The physiological evidence indicating that polarized light is detected primarily by UV and B photoreceptors was complemented by the observation of orthogonally arranged microvilli in anatomical cross-sections of the retina, which might belong to polarization-opponent photoreceptor pairs with orthogonal sensitivity maxima to polarized light. Behavioural tests in a Y-maze demonstrated that starved spittlebugs preferred linearly polarized over a diffuse visual stimulus. This preference disappeared when a yellow filter blocked UV and blue light, implicating the necessity of UV and B photoreceptors for the detection of polarized reflections. Our findings demonstrate that *P. spumarius* uses visual cues, including polarized light, which may

aid in the visual detection of reflections from host plants. Understanding these visual mechanisms provides new insight into the ecology of this key vector species and may inform strategies to disrupt its host-finding behaviour.

KEYWORDS
host finding, insect behaviour, polarotaxis, trichromatic vision, visual acuity, visual system

1 | INTRODUCTION

Insects rely on vision and olfaction as primary sensory modalities for locating host plants, and these cues shape interactions across a wide range of agroecosystems (Avosani et al., 2024). Within the Auchenorrhyncha, these senses are especially important for long-distance host localization, yet the role of vision has received far less attention compared to olfaction.

Insects' vision is mediated by compound eyes, which are image-forming organs composed of numerous ommatidia, each sampling a narrow part of the visual field (Land & Nilsson, 2012; Rayer et al., 1990). This modular design allows insects to function across environments ranging from bright daylight to dim twilight and moonlight, underpinning a wide range of visually guided behaviours (Land & Fernald, 1992; Nilsson & Warrant, 1999). Within each ommatidium, photoreceptor cells contain opsins in their microvillar membranes, converting light into neural signals (Chittka & Menzel, 1992). The number and spectral sensitivity of photoreceptor types vary widely across insects, from a single receptor class in specialized eye regions (Gogala, 1967) to five in flies or as many as 15 in butterflies (Briscoe, 2000; Chen et al., 2016; Hardie, 1986; Ogawa et al., 2013). This diversity enables complex colour vision, with spectral sensitivity extending from below 300 nm into the red range beyond 700 nm (Briscoe & Chittka, 2001). Across insects, a conserved ancestral set of ultraviolet-, blue-, and green-sensitive receptors is shared across many taxa (Briscoe et al., 2003; Briscoe & Chittka, 2001; Bruckmoser, 1968; Chittka, 1997; Hariyama et al., 1993; Ichikawa & Tateda, 1982; Kinoshita et al., 1997; Seki & Vogt, 1998; van der Kooi et al., 2021; White et al., 1994). This ancestral arrangement has frequently been modified into specialized colour vision systems adapted to ecological demands (Arikawa et al., 1987; Bernard & Remington, 1991; Chittka, 1997; Seki & Vogt, 1998).

In addition to their ability to detect contrasts in light intensity or colour, insects have also evolved mechanisms to detect linearly polarized light. This capability is widespread among insects and plays an ecologically significant role in navigation and host detection. Light from natural sources is mostly diffuse or unpolarized, meaning that the electric fields of light photons are randomly aligned. However, light scattered from atmospheric particles or reflected from smooth, non-metallic surfaces becomes polarized, that is, the electric fields of photons predominantly oscillate in one plane. Celestial polarization patterns provide a wide-field orientation cue (Labhart & Wehner, 2006), while reflections from surfaces such as water, leaves, or animal cuticles produce local polarized signals, with water providing a consistent source of horizontally polarized light (Wehner, 2001). The physiological basis for polarization sensitivity (PS) lies in the alignment of photoreceptor microvilli, which preferentially absorb photons with electric vectors parallel to their long axis (Roberts et al., 2011; Wehner, 1976). Insects detect the angle and degree of polarization (AoP and DoLP) by comparing responses from photoreceptors with differing (orthogonal) microvillar orientations within the same visual field (Marshall & Cronin, 2011; Wehner, 2001, 2014). Polarization vision is mediated by photoreceptor pairs and polarization-opponent coding, that is, comparison of signals from receptor pairs via mutual synaptic inhibition (Heras & Laughlin, 2017; Homberg, 2015; Labhart & Meyer, 1999). Beyond navigation, insects exploit non-celestial polarization cues for tasks such as water finding and host-plant selection. While early studies emphasized plant colour, brightness, and shape in host selection (Prokopy & Owens, 1983; Reeves, 2011), recent research shows that DoLP differences between host and non-host plants can provide an additional or even more reliable cue (Blake et al., 2019; Foster et al., 2018). Reflections from leaves are polarized due to specular reflection from the cuticle, with DoLP and AoP influenced by surface properties like wax layers, pubescence, and pigmentation (Foster et al., 2018; Grant et al., 1993; Maxwell et al., 2016). Polarization cues remain effective under varying illumination conditions, including shade, and changing solar angles, where colour signals may get degraded (Foster et al., 2018). While neural pathways for celestial polarization are well-characterized (Homberg, 2015), those mediating non-celestial polarization-guided behaviours are less explored (Heinloth et al., 2018).

Beyond spectral and PS, another key determinant of visual performance is spatial resolving power, or visual acuity. Visual acuity is commonly expressed as the photoreceptor acceptance angle ($\Delta\varphi$), usually equal to or slightly larger than the interommatidial angle ($\Delta\rho$), both shaped by facet diameter and eye curvature (Kirwan et al., 2018; Land, 1997). These parameters determine how well insects can resolve spatial detail, with trade-offs between resolution and field of view. z Predators and species seeking conspecifics often evolve frontal acute zones with high resolution (Rossel, 1980; Sherk, 1977), while herbivores typically prioritize wide visual coverage to improve threat detection (Horridge, 1978; Land, 1989, 1997). Compound eyes thus underpin behaviours such as foraging, navigation, and predator avoidance, with direct implications for pest management through manipulation of visual cues (Döring, 2014).

Understanding the role of visual cues in the interaction with the surroundings for a given insect species is therefore essential, not only for clarifying their sensory ecology but also for developing sustainable

pest management strategies. Indeed, for insect species that rely heavily on visual cues to locate host plants within agroecosystems, the use of repellent or attractant visual stimuli offers a promising avenue for disrupting pest–plant interactions (Antignus et al., 2001; Athanasiadou et al., 2024). This approach could be particularly valuable in managing vector-borne plant pathogens, where chemical control of vectors often yields inconsistent reductions in disease transmission risk (Daugherty et al., 2015). By reducing insect–plant encounters through interference with visually driven host location, it may be possible to limit pathogen spread effectively. To assess how vision can be exploited in this context, it is first necessary to understand the structure and functional diversity of insect visual systems. Conventional traps have typically been designed around human-defined colours and shapes, yet these often fail to capture cues that are highly salient to insects, such as ultraviolet or polarized reflections (Ben-Yakir, 2020; Santer & Allen, 2024; van der Kooi et al., 2021).

The meadow spittlebug *Philaenus spumarius* L. (1758) (Hemiptera: Aphrophoridae) has recently emerged as a key threat for European agriculture and landscape given its primary role in the epidemiology of the xylem-limited bacterium *Xylella fastidiosa* (Cornara et al., 2017; Cruaud et al., 2018; Moralejo et al., 2019; Rodrigues et al., 2022). The meadow spittlebug is a highly polyphagous and widely distributed species, ranging from the Mediterranean to the Nearctic regions (Thompson et al., 2023). The extreme polyphagy and the frequent dispersal of spittlebug adults between different landscape compartments make the management of *X. fastidiosa* a major challenge in affected ecosystems. Indeed, the bacterium is transmitted by insect vectors in a persistent propagative non-circulative manner, with a relatively short contact between vectors and source and recipient plants being sufficient for pathogen transmission (Cornara et al., 2024; Purcell & Finlay, 1979). This transmission dynamic limits the options available for effective pathogen control, with successful management achievable primarily through disruption of host location cues to prevent insect landing on the host plant. However, relatively little is known about the sensory mechanisms underlying host location by *P. spumarius*. Most studies have focused on olfactory cues, often yielding inconsistent results, while the role of visual perception remains largely understudied (Anastasaki et al., 2021; Cascone et al., 2022; Germinara et al., 2017; Ranieri et al., 2016; Rodrigues et al., 2022). On the other hand, aside from a study on the general structure of the compound eyes and their post-embryonic development (Keskinen & Meyer-Rochow, 2004), no dedicated research has addressed the role or significance of vision and visual cues in the interactions of *P. spumarius* with other organisms, including host plants.

In the present study, we investigated the visual capabilities of the meadow spittlebug *P. spumarius*, aiming to comprehensively characterize their colour and polarization vision, along with the structures that enable these visual functions and determine visual acuity. The research integrates electrophysiological measurements, anatomical analysis, optical measurements of visual acuity, and a dual-choice behavioural experiment in a Y-maze to examine the architecture and functionality of the visual system, as well as its influence on behaviour.

2 | MATERIALS AND METHODS

2.1 | Spittlebug collection and maintenance

We collected adult spittlebugs in the meadows in the Ljubljana region from June to October using sweep nets (20–30 individuals were collected every second week). The spittlebugs were transferred to shaded cages (90 × 60 × 60cm Pop-up Cage, Watkins & Doncaster) kept outside (June: mean temp.: 21.8°C and rainfall: 238.2 mm; July: mean temp.: 25.7°C, rainfall: 39 mm; August: mean temp.: 26.0°C, rainfall: 107.2 mm; September: mean temp.: 18.8°C, rainfall: 265 mm). The plants used as a food source were 3- to 6-week-old basil plants (*Ocimum basilicum* L.) (seeds and seedlings from Flanca d.o.o., Voglje, Slovenia), which were replaced every 2 weeks and watered as needed to maintain adequate soil moisture.

2.2 | Anatomical analysis

2.2.1 | X-ray micro-CT imaging

We analysed x-ray micro-CT scans of *P. spumarius* obtained at the beamline 8.3.2, a high-resolution synchrotron-based microtomography facility at the Advanced Light Source (Lawrence Berkeley National Laboratory, USA). This beamline is designed specifically for 3D imaging of biological and material specimens with submicron resolution. Scans were performed following the methodology detailed in Clark et al. (2023). Specimens were prepared according to Wood and Parkinson (2019), including ethanol storage, Lugol's staining, and scanning within a sealed pipette tip. Scanning was performed with a 4× objective lens, generating approximately 1750 images per specimen, which were reconstructed into 3D volumes with a voxel size of 1.605 µm (Gürsoy et al., 2014).

The acquired dataset included the entire head along with surrounding tissues. For this study, we digitally isolated the retina of a single spittlebug using segmentation techniques. A semiautomated volume thresholding tool was applied to demarcate different anatomical structures, followed by manual data marking and extraction. Visualization and further analysis were conducted using Dragonfly v. 2021.3 (Object Research Systems, Canada). The rhabdoms could not be resolved in the micro-CT data; thus, we examined their architecture using light microscopy and 3D reconstruction.

2.2.2 | Light microscopy, 3D reconstruction and TEM of the eye

For light and transmission electron microscopy (TEM), eye samples from one male and one female spittlebug were fixed in a solution of

3.5% glutaraldehyde and 4% paraformaldehyde, followed by post-fixation in 1% osmium tetroxide. After dehydration in a graded ethanol series and propylene oxide, the samples were embedded in Spurr resin using a gradual infiltration process over 2 days. Semi-thin (1 μm) and ultra-thin (50–70 nm) sections were obtained using an Ultracut S ultramicrotome (Leica, Germany) with a diamond knife (Diatome, Switzerland) and stained by the Richardson technique with a blue dye (semi-thin) or uranyl acetate and lead citrate (ultra-thin sections) before imaging (for detailed procedure see Supplement). Ultra-thin sections were examined using a Talos L120C TEM (Thermo Fisher, USA) at 1600×, 3400×, 6700×, and 17,500× magnification. Semi-thin consecutive sections were observed under 200x magnification with an Axio Imager M.2 (Zeiss, Germany), capturing ~180 images via an RGB camera (Blackfly BFS-U3-200S6C-C, Teledyne, USA).

Microscopy images were analysed to identify structural features and measure corneal lenses, crystalline cones, and rhabdom diameters. TEM imaging provided crystalline cone and medial rhabdom diameter measurements and examined microvillar structures. For 3D reconstruction, semi-thin section images of the left eye were manually registered and automatically aligned (rigid transformation) using ImageJ v. 2.14.0/1.54f (Schindelin et al., 2012) with TrakEM2 (Cardona et al., 2012). Damaged sections were replaced with duplicates of neighbouring sections. The aligned images were imported into Dragonfly v. 2022.2 (ORS) for 3D reconstruction, where individual ommatidia components were segmented and labelled to visualize internal architecture. Segmentation was performed in three planes, focusing on two concentric levels of ommatidia surrounding the central one. In the outer concentric regions, one or two ommatidia were left unsegmented between each segmented one to reduce redundancy and simplify visualization. Although the reconstruction provided a detailed spatial representation of the ommatidia (Figure 2), some distortions were present due to imperfections in the semi-thin sections and possible specimen shrinkage during fixation. Skewing of ommatidia and rhabdoms was particularly noted near the eye margins. Therefore, anatomical tracing (Figure S1) was considered insufficient for accurate quantitative estimation of optical axes or visual resolution.

2.2.3 | Measurements of interommatidial angles

Distortions in the anatomical reconstructions prevented reliable optical-axis estimates, so interommatidial angles were instead measured optically by tracking facet displacement above the pseudopupil, following the method of Franceschini and Kirschfeld (1971), Stavenga (1975), and Horridge (1978). The pseudopupil is an optical phenomenon seen in ommatidia whose optical axes align with the objective lens aperture; these facets appear dark because incident light is absorbed in the rhabdoms (Franceschini & Kirschfeld, 1971; Land, 1997). By rotating the eye in 5° increments and keeping the pseudopupil centred, the number of facets (N) crossing over it can be counted, allowing calculation of the local interommatidial angle as $\Delta\rho = 5°/N$. Measurements were taken in three anatomical planes: antero-posterior (A–P), dorso-ventral (D–V), and diagonal (AD–VP). We employed a modified tele-microscopic system (Pirih et al., 2020), originally developed for butterfly eyeshine imaging. The epi-illumination microscope included a shortened telescopic tube and UV-capable crossed polarizing filters (Bolder Vision Optik, USA) to reduce corneal reflections and enhance pseudopupil visibility. The eye was illuminated with wide-spectrum white light. A spittlebug was immobilized on a pipette tip and positioned in a goniometric stage so that the eye's centre aligned with the main objective lens focal point. The pseudopupil was first located in the anterior eye corner, and the goniometer was moved in 5° steps laterally, vertically, and diagonally. Image stacks were imported into ImageJ, aligned, and analysed using the Plot Profile function to determine the pseudopupil centre. Displacement of reference ommatidia relative to this centre was calculated across image frames. Each measurement was repeated five times using different reference ommatidia, and the results were averaged. A custom MATLAB script (v. R2021a, MathWorks, USA) interpolated values for non-measured facets, applied a Gaussian filter ($\sigma = 1.5$) for smoothing, and generated a heatmap overlaid on the micro-CT-based retinal map.

2.3 | Electrophysiological measurements

2.3.1 | Single-cell recording

Spittlebugs actively feeding on plant material were selected for measurements. Their legs were secured with a beeswax-resin mixture, and the insect was positioned dorsal-side down in a plastic holder at a 45° angle. The holder was mounted on a small goniometer, placed into a larger goniometer, and adjusted to align the eye at the centre of rotation. A reference electrode (Ag/AgCl, 50 μm) was inserted into the opposite eye. A small rectangular opening in the posterior eye cuticle allowed the insertion of a glass electrode through the cornea, sealed with silicone paste to prevent drying. Sharp borosilicate microelectrodes (1 mm/0.5 mm) were pulled using a P-2000 horizontal puller (Sutter, USA), filled with 2 M KCl (150–250 MΩ resistance), and attached to a 100 μm Ag/AgCl wire in a plastic holder. The measuring electrode, reference, and ground were connected to a preamplifier mounted on the larger goniometer, which was enclosed in a three-sided black Faraday cage shielding against stray light. A piezo micromanipulator (Sensapex, Finland) moved the sharp electrode through the pre-cut hole in 1.5 μm steps. Penetration of receptor cells was indicated by a drop in electrical potential and the appearance of a light-evoked receptor potential. Signals were amplified using a high-impedance SEC-10LX amplifier (NPI, Germany) in bridge mode, digitized via a CED1401 micro MK2 interface (Cambridge Electronic Design, UK), and recorded with WinWCP 5.5.4 (University of Strathclyde, Scotland). The experimental setup follows the methodology described by Belušič et al. (2025) (Figure S2).

Light stimulation came from two sources. The first was a 75 W xenon arc lamp (Cairn Research, UK), filtered by a monochromator (BandM Optik, Germany), a mechanical shutter, and a motorized, continuously graded neutral density (optical density 0–4) filter (Thorlabs,

Germany), and projected into an optical fibre. Additional adjustments were made using discrete neutral density filters (0.5–3.2 log units). All optical elements were UV-capable (quartz or fused silica). The second source was the 'LED synth' setup, with 21 LEDs peaking between 365 and 685 nm, spaced at 15 nm intervals (Belušič et al., 2016). A combination of diodes and a diffraction grating enabled spectrum selection with 15 nm precision. Light from both sources was projected coaxially onto the insect eye, shaped using a field and aperture diaphragm. A radiometrically calibrated spectrophotometer (Flame, Ocean Optics, USA) ensured both sources emitted equal photon flux density at all wavelengths (max. 1.5×10^{15} photons cm^{-2} s^{-1}). For PS measurements, a UV-capable polarizer (OUV2500, Knight Optical, UK) was inserted into the monochromator's beam on a motorized holder. All stimulation devices were controlled by Arduino Uno and Due microcontrollers (Arduino, Italy).

2.3.2 | Spectral sensitivity measurements

As the electrode moved through the retina, the receptor cell type was identified from the spectral profile of responses to rapid flashes from the 'LED Synth' system. Spectral sensitivity was then measured using a computer-controlled monochromator, delivering 300-ms flashes at 1-s intervals. The stimulus wavelength was stepped from 300 to 700 nm in 5 nm increments, and the final spectral sensitivity was averaged from both curves.

2.3.3 | Intensity-dependence of response measurements

After spectral sensitivity measurements, an intensity-response curve was recorded at the maximally efficient wavelength (λ_{max}). The monochromator beam was set to λ_{max} and dimmed with a neutral density filter over 4 log units. 300-ms flashes were delivered at increasing intensity in 0.2 log steps, with 2-s intervals.

2.3.4 | Measurement of polarization sensitivity

PS was measured at λ_{max} by inserting a motorized linear polarizing filter OUV2500 (Knight Optical, UK) in the optical axis of the monochromator. Using neutral density filters, we adjusted the light intensity to elicit signals within the amplitude range corresponding to the steepest part of the intensity-response curve. Between consecutive flashes, the polarizer was rotated in 18° increments, completing two full rotations.

2.3.5 | Data processing for spectral sensitivity, intensity, and PS

Measurement data from spectral sensitivity, intensity, and PS (WinWCP software) were exported to a spreadsheet and processed in MATLAB (MathWorks, USA). A sigmoidal (Hill) curve was fitted to intensity-response voltages to determine the slope, centre, and maximal depolarization. Spectral and polarization voltages were transformed into sensitivity values via the reverse Hill transformation, following the method described by Belušič et al. (2017), by calculating the stimulus intensity required to elicit a fixed, low-level response amplitude at each wavelength or polarization angle. PS was evaluated by fitting a cosine-squared ($\cos^2$) function to the data, with PS calculated as the ratio of the function's maximum to minimum response. The angle of maximal sensitivity (φ_{max}) was defined at the two peaks of the fitted function, separated by the 180° rotation of the polarizer. φ_{max} indicates the angle of linear polarization at which the photoreceptor produces its maximal response. Following our previous results (Meglič et al., 2019), photoreceptors with PS < 2, 2 < PS < 4, and PS > 4 were categorized as having low, modest, or high PS, respectively. Namely, green-sensitive R1-6 photoreceptors of polarotactic horseflies have PS minimized to *low* (PS ∼ 1.1–2.0) through systematic microvillar misalignment (twisting) but do not contribute to polarization vision; their UV or green-sensitive R7y and R8y receptors have a *modest* PS ∼ 2–3 and do not contribute polarization vision, whereas their UV and blue-sensitive R7p and R8p have a *high* PS (PS > 3) and are the main substrate for polarization vision. Data processing and visualization were done in Prism 8.0 (GraphPad, USA).

2.4 | Behavioural tests of polarotaxis

In August 2024, we conducted behavioural assays to examine whether *P. spumarius* responds to horizontally polarized light. Light reflected from leaf surfaces becomes partially polarized via specular reflection, resulting in predominantly oblique or horizontal polarization under natural illumination geometries (Blake et al., 2019; Foster et al., 2018). From the subjective perspective of an insect walking on a plant leaf, the reflections are horizontally polarized. We therefore restricted our behavioural tests to horizontal linear polarization, which serves as a plausible representation of ecologically relevant foliar reflections. To test its potential role in spittlebug decision-making, we employed a dual-choice setup using a Y-shaped arena (main tunnel: 12 cm wide × 40 cm long; side tunnels: 12 cm wide × 30 cm long; Figure S2). To eliminate polarized reflections and provide grip, walls and ceiling were lined with rough filtration paper. A barrier with a slit was positioned 20 cm inside each side tunnel, with 45° mirrors behind them reflecting light from a 300 W WASP wide-spectrum source (HIVE LIGHTNING Inc., USA). This lamp model, no longer available commercially, is based on microwave-induced plasma in a Xe-filled quartz ampoule and emits a flicker-free 300–700 nm spectrum, resembling sunlight (Figures S4 and S5).

Two visual stimuli were used: diffuse and horizontally polarized light. Both were generated by passing light through a two-layered diffuser (two layers of objective cleaning paper, Whatman, USA, and a glass diffuser, Thorlabs, Germany) and a polarizer (UV-capable, Bolder Vision Optik, USA) positioned between the barrier and the light source. Diffuse light passed through the polarizer first, then the

diffuser, while polarized light passed through in reverse order. This ensured similar light intensity in both conditions, with polarization set at 0% or 100%. Before the experiments, the maze was inspected with a monochrome polarimetric Phoenix camera (Lucid Vision, Germany), fitted with a quartz lens (Ricoh, Japan) and Techspec 50 nm bandpass filters peaking at 350, 450, and 550 nm (Edmund Optics, UK) for any uncontrolled reflections of polarized light from the walls. In a preliminary test, we observed that field-collected spittlebugs approached the stimuli randomly. No statistical analysis was conducted for these initial trials, as the goal was to observe general orientation behaviour under natural feeding conditions. Based on these observations, we hypothesized that starving the insects before testing would elicit more active host-seeking behaviour and potentially reveal directional preferences. Based on preliminary trials, the time point of 3 min allowed sufficient opportunity for a decision to be made while minimizing the likelihood of reversal. In total, 103 spittlebugs with unique IDs were used across both experiments (39 males and 64 females). These insects were distributed and tested in 7 days (tests), 10–20 at a time. Starvation and acclimation were conducted individually under ambient light conditions, without access to plants or water. After the starvation period, each insect was separately placed at the entrance of a Y-shaped arena and covered to ensure that the surrounding light would not influence their choice. After 3 min, the cover was removed, and the insect's choice was observed. If a jump sound was heard, the choice was recorded immediately, since it resulted in a choice being made, and waiting for the 3-min mark could result in the change of the choice. If the spittlebug remained in the main tunnel or stopped between the two arms of the Y, it was classified as 'passive'. To control for potential sources of bias, such as lighting asymmetry, temperature differences, chemical cues, or spatial learning, stimuli were systematically swapped between the left and right arms of the arena after each full measurement set. Each spittlebug was tested once per stimulus arrangement (set). After all insects had been tested, the positions of the stimuli were swapped, and the same insects were tested again. Thus, each individual contributed two observations per test. For the first set of tests, spittlebugs were starved and dehydrated for 3 h, while in the second set, this period was extended to 4 h. In total, 182 choices were recorded in the first experiment. Testing took place daily between 1:00 PM and 4:00 PM, with two sets completed per day (test). Each spittlebug was assigned a unique ID to track repeated behaviour. The sex of the insects and the position of the stimuli were also recorded. The first experiment employed a broad-spectrum light source, while the second used the same setup with an added blue-attenuating filter (Lee 101, Lee Filters, USA) mounted on UV-blocking plexiglass. The spectral output and intensity profiles of both the unfiltered and filtered light sources are provided in Figure S4. The spectral restriction was intended to keep the UV and B photoreceptors, which have high PS, deprived of stimulation while allowing the insects to be guided primarily by the G photoreceptors, which have low PS, as suggested by electrophysiological data (Figure 5b,c). In the second experiment, only nine spittlebugs were tested in two sets under the original wide-spectrum condition, and the same insects in two sets under the filtered condition, resulting in a total of 36 recorded choices. Statistical analysis was performed using R version 4.4.2 (R Core Team, 2020). To assess stimulus preference in both experiments, we modelled the binary response variable, representing the choice between polarized and diffused stimuli, using a generalized linear mixed model (GLMM) with a binomial distribution and logit link function. Insects that did not make a choice (passive) were excluded from the analysis. The model included insect sex as a fixed effect, while random intercepts were specified for experimental repetition (Test) and individual insect ID to account for unpredictable variation between experimental replicates and repeated measurements within individuals. For the second experiment, we have used the same model. It included Test (light condition) as a fixed effect, and a random intercept for individual ID (Index) to account for repeated measurements within insects. Due to the small sample size, results should be interpreted with caution. Model fitting was performed using the glmmTMB package (Brooks et al., 2017), and residual diagnostics were conducted using the DHARMa package (Hartig, 2016).

3 | RESULTS

3.1 | Anatomy of the spittlebug eyes

Each compound eye of the spittlebug consists of approximately 600–800 ommatidia, as previously reported by Keskinen and Meyer-Rochow (2004). This range is supported by our observations, where two independent counts based on light microscopy images yielded ommatidia numbers within this interval. Measurement of diameters of ommatidial structures, such as corneal lenses, crystalline cones, and rhabdoms (Figure S3), measured on semi-thin sections revealed no differences between the male and female insect. The 3D model, reconstructed from micro-CT sections, shows that the external curvature of the eye somewhat deviates from a spherical shape (Figure 1). When viewed along the sagittal plane, the ommatidia are assembled in concentric circles around the central ommatidium (Figure 2—rhabdom marked with yellow colour). In the coronal plane, the anterior and central part of the eye is flattened (Figure 1b), meaning that the eye radius gradually decreases from the anterior to the posterior part of the eye. Flat parts of compound eyes are indicative of acute zones with minimal interommatidial angles. However, the viewing angles of the ommatidia depend not only on the eye curvature but also on the optical coupling of the rhabdoms and the dioptrical apparatus. If the rhabdoms are skewed, then the viewing angles are not radial to the local curvature of the cornea. Across the sections, the ommatidia appear to maintain a consistent packing density and uniform arrangement, suggesting a relatively homogeneous visual field without distinct high-acuity zones. A 3D reconstruction was then made of aligned images of serial sections (Figure 2). We can observe that the vertical alignment of the corneal lens, crystalline cone, and rhabdom decreases from the central part of the eye to the outer margins.

Interommatidial angle measurements revealed spatial variation across the compound eye (Figure 1c). The average $\Delta\rho$ across all measured regions was approximately 6.15°, indicating relatively coarse spatial resolution overall (Figure 3b). However, local values ranged from a minimum of 4° to a maximum of 10°, with the smallest angles

observed near the central dorsal–ventral (D–V) axis. This pattern suggests the presence of a modestly developed acute zone, offering slightly finer resolution in the anterior and central part of the visual field. Along the antero–posterior (A–P) axis, Δρ values increased towards the posterior margin, reaching up to 10°, indicating reduced sampling density in rear-facing regions. The diagonal (AD–VP) axis displayed intermediate values. These measurements reflect smooth spatial gradients rather than sharply bounded zones.

The ommatidial ultrastructure was further examined with TEM to observe the spatial alignment of microvilli within the rhabdoms. We obtained cross-section images of the retina at various depths and confirmed that the arrangement of receptor cells and microvillar structures exhibits minimal heterogeneity along the Z-axis, indicating a uniform organization within each ommatidium. The semithin and ultrathin cross-sectional images (Figure 4) revealed thick rhabdoms with a diameter of ~2.80 μm (within the boundaries of the palisades), indicative of a wide acceptance angle Δφ, matching the large interommatidial angle Δρ and maximizing light gain (Figure 4b,c). The rhabdoms were surrounded by palisades and screening pigment granules, both typical for spittlebug eyes (Keskinen & Meyer-Rochow, 2004) (Figure 4c). The rhabdoms also contained pairs of rhabdomeres with orthogonally oriented microvilli, a possible specialization for polarization vision (Figure 4d).

3.2 | Intracellular recordings in the photoreceptors

We measured the spectral ($N = 41$, 11 M and 30F) and PS (N = 41, 11 M and 30 F) of photoreceptors in both male and female specimens of the meadow spittlebug. The photoreceptor sensitivity peaks (λ_{max}) were at 340–350 nm, 440–450 nm, and 520–530 nm, indicating three spectral classes: UV, blue (B), and green-sensitive (G) (Figure 5a), ancestral organization, typical for many taxonomic groups of insects (va der Kooi et al., 2021). We observed no difference between the sexes in terms of spectral sensitivity peak or PS magnitude or angle of the peak response; therefore, the results were merged for all subsequent analyses.

The PS ratio PS was low in G photoreceptors (mean = 1.44, SD = 0.42) but high in most of the UV (mean = 5.71; SD = 3.12) and B (mean = 9.99; SD = 9.79) photoreceptors (Figure 5b–d). Some PS values in UV and B receptors were very high (PS > 10), indicating receptor subclasses that provide lower PS, suitable for stable colour vision, or high PS, which is an appropriate substrate for polarization vision. The UV photoreceptors had mostly vertical sensitivity maxima (φ_{max}), while the B photoreceptors had φ_{max} that displayed no clear dominant orientation.

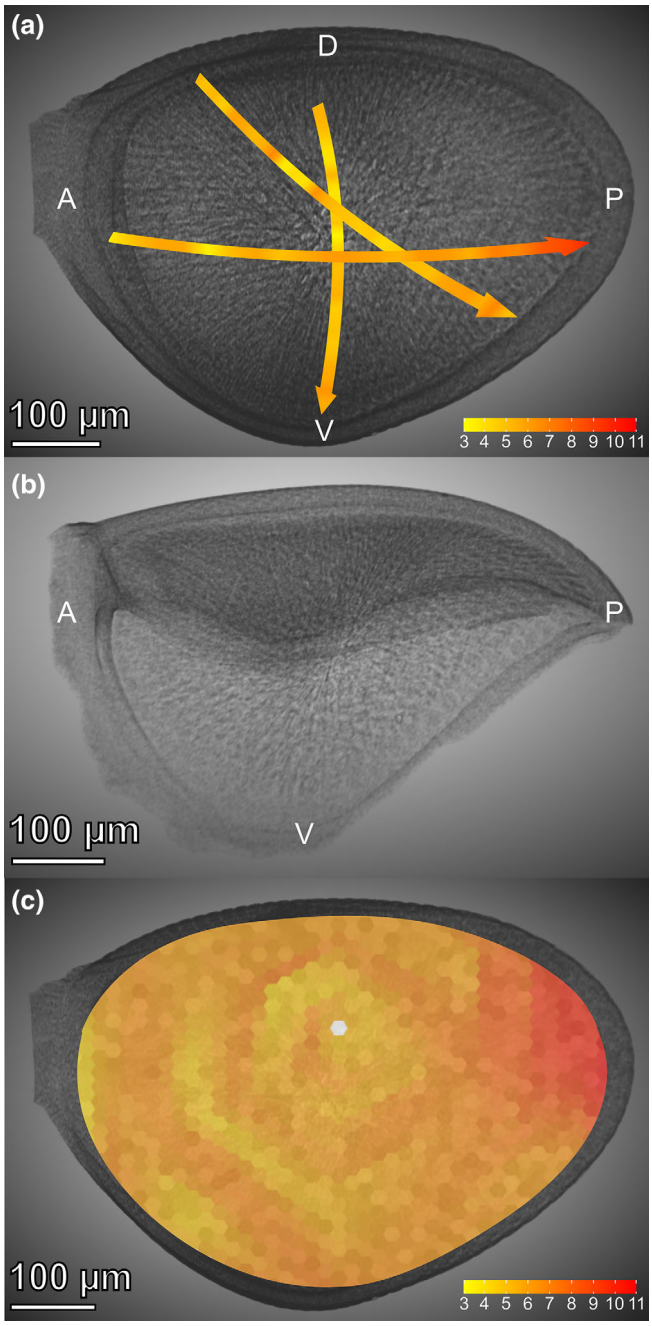

FIGURE 1 Left compound eye of the spittlebug, reconstructed using images from x-ray microtomography, (a) sagittal view and (b) ventral view, with the central part opposite to the ventral marking (V). Colours in (a) indicate the interommatidial angles, measured optically along three planes. In panel (c), interommatidial angles interpolated from optical measurements, coded with colour. Directions: A, anterior; P, posterior; D, dorsal; V, ventral.

3.3 | Behavioural tests of polarotaxis

Philaenus spumarius was tested in a Y-maze to determine whether it could guide its locomotion based on the detection of linearly polarized light. Starved individuals were allowed to choose between two backilluminated arms of the maze with matched light intensity. In one arm, they were exposed to horizontally polarized, broad-spectrum ('white') light. In the other arm, they could view diffuse, broad-spectrum light. A total of 161 active choices, between 103 spittlebugs, were analysed across seven tests (Figure 6a). Since only 7.76% of spittlebugs remained passive, they were excluded from the final analysis. The

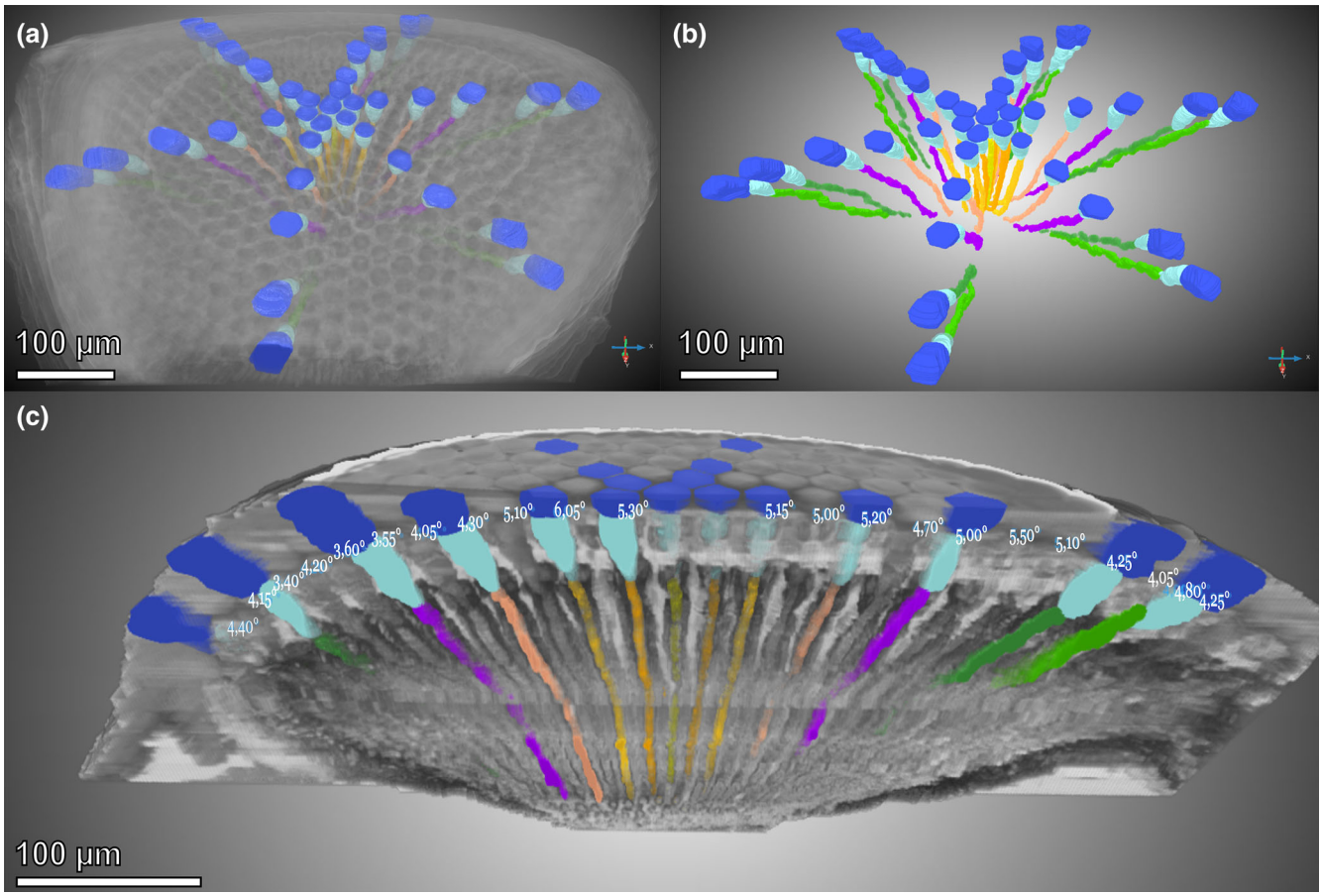

FIGURE 2 3D representation of the spittlebug left eye, reconstructed from semithin sections, observed with a light microscope, and segmented. The colours in the figures represent: Dark blue—corneal lenses, light blue—crystalline cones, and other colours—ommatidial rhabdoms equidistant from the centre of the eye. (a,b) Sagittal view of the reconstruction (anterior—left, posterior—right). (c) Cross-section in the coronal plane, with measurements of interommatidial angles, derived from anatomical tracing.

effect of sex on stimulus choice was not statistically significant ($z = -0.599$, $p = .549$) with females exhibiting an estimated polarized choice probability of 0.703 (SE = 0.0574; 95% CI: 0.580–0.802) and males 0.654 (SE = 0.0776; 95% CI: 0.491–0.788), indicating no meaningful difference between males and females in their likelihood of choosing the polarized stimulus. The model intercept was significantly positive (estimate = 0.8597, SE = 0.2748, z value = 3.129, $p = .00176$), indicating a strong overall preference for the polarized stimulus. The marginal mean probability of choosing polarized light was estimated at 0.687 (SE = 0.0522; 95% CI: 0.577–0.779). The variance attributed to Test was 0.195 (SD = 0.441), while the variance for ID was negligible (5.6×10^{-9}). Model assumptions were validated using simulated residuals via the DHARMa package. Model diagnostics indicated no evidence of overdispersion (DHARMa dispersion = 1.004, $p = .968$), and a significant effect of Test was detected ($\chi^2 = 12.693$, $df = 6$, $p = .048$), suggesting that the test session contributed to variation in stimulus choice. The model was fitted using a binomial distribution with a logit link (AIC = 206.5, BIC = 218.8, $N = 161$). The residuals did not deviate from a uniform distribution, and no overdispersion was observed. Additionally, the outlier test did not indicate any extreme values.

In the second behavioural test, the spittlebugs pooled by sex could choose between polarized and diffused light under two distinct spectral conditions: a broad-spectrum light condition and a yellow-restricted spectral condition. Each of the nine spittlebugs contributed four choices, resulting in 36 observations in total. Statistical modelling with a binomial GLMM indicated that the difference between the two spectral conditions was not statistically significant ($\chi^2 = 0.85$, $df = 1$, $p = .356$; Wald test). The variance explained by individual ID was negligible (Var = 2.9×10^{-9}). DHARMa residual diagnostics showed no evidence of overdispersion (dispersion = 1.028, $p = .936$). Still, estimated probabilities indicated a higher tendency to choose the polarized stimulus under broad-spectrum conditions (0.688 ± 0.116 SE; 95% CI: 0.433–0.864) than under yellow-restricted light (0.529 ± 0.121 SE; 95% CI: 0.303–0.745). The odds ratio of choosing polarized light between the two conditions was 1.96 (SE = 1.42, z = 0.924, $p = .356$). These results, while preliminary, suggest a possible reduction in polarized-light preference when UV and blue photoreceptor input was attenuated (Figure 6b).

These preliminary results indicate a potential reduction in polarized-light preference when UV and blue photoreceptor input was attenuated, consistent with the hypothesis derived from our

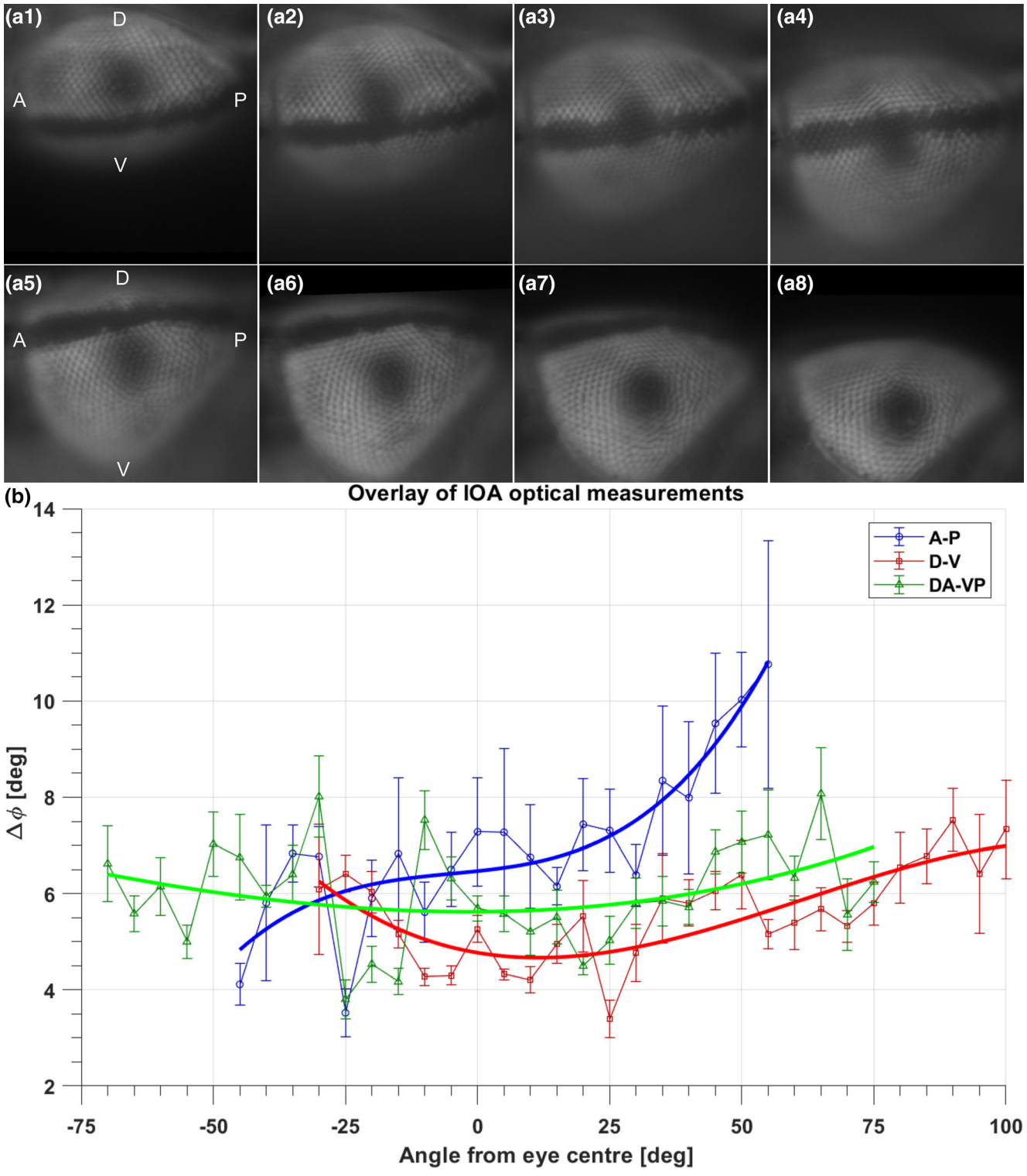

FIGURE 3 Optical mapping of interommatidial angles—a sample of eight images (a1–a8). Facets and pseudopupil (dark spot in the centre) were observed at different angles across the dorso-ventral plane, in 5° steps. (b) Calculated interommatidial angles across three planes (A-P, antero-posterior; D-V, dorso-ventral; DA-VP, diagonal from dorso-anterior to ventro-posterior). The dark stripe across the eye is due to pigmentation in the cornea.

electrophysiological data that these receptors contribute to polarization vision in *P. spumarius*. However, given the limited sample size and non-significant differences between treatments, the evidence remains inconclusive. Further experiments with larger sample sizes are needed to confirm whether UV and blue receptors play a central role in polarization-guided behaviour.

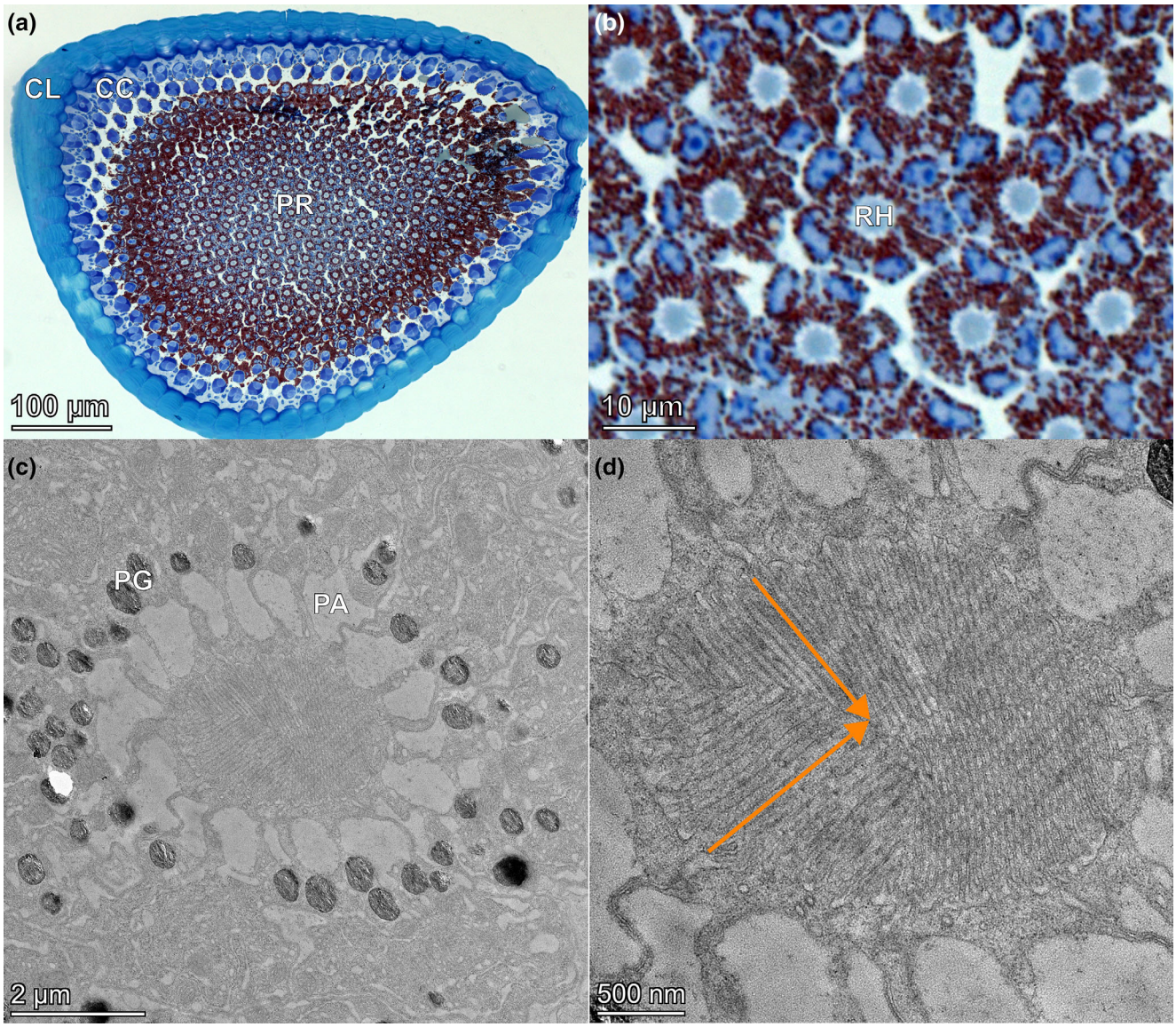

FIGURE 4 Sagittal cross-section of the spittlebug eye. Panels (a,b), semithin sections at 85 µm from the cornea. Panels (c,d) ultrathin sections, observed with transmission electron microscope. CL, corneal lens; CC, crystalline cone; PR, photoreceptors; RH, rhabdom; PA, palisades; PG, pigment granules. Orange arrows in D indicate a rhabdomere pair with orthogonally oriented microvilli.

4 | DISCUSSION

The meadow spittlebug *P. spumarius* is the main European vector of *X. fastidiosa*. Host location by the insect vector is a critical step in the pathogen transmission cycle, enabling the pathogen to escape from infected hosts and spread within the environment. Understanding the sensory basis of host location, that is, the key cues guiding an insect species towards a plant, could provide opportunities to disrupt host–vector interactions and ultimately reduce the risk of pathogen transmission. In *P. spumarius*, the sensory mechanisms underlying host location remain poorly understood. Research on the role of olfactory cues in plant detection has yielded inconsistent results, while the contribution of visual cues has largely been overlooked.

In this study, we characterized the visual system of *P. spumarius* through electrophysiological, anatomical, and behavioural approaches. Our results provide evidence for trichromatic colour vision, PS, and moderate spatial resolution. These visual capabilities, together with the polarotactic behaviours observed in controlled experiments, indicate that vision likely plays a functional role in guiding locomotion and influencing behavioural decisions. For agricultural pests such as aphids, whiteflies, and leafhoppers, visual cues may complement or even supersede olfactory cues in the host location process (Antignus, 2000; Ben-Yakir et al., 2013; Blake et al., 2019; Coombe, 1981; van der Kooi et al., 2021). Despite this, visual inputs remain relatively understudied compared to chemical stimuli. Yet, a detailed understanding of how pests exploit visual information is essential for developing strategies to disrupt insect–plant interactions and reduce the risk of vector-borne pathogen transmission.

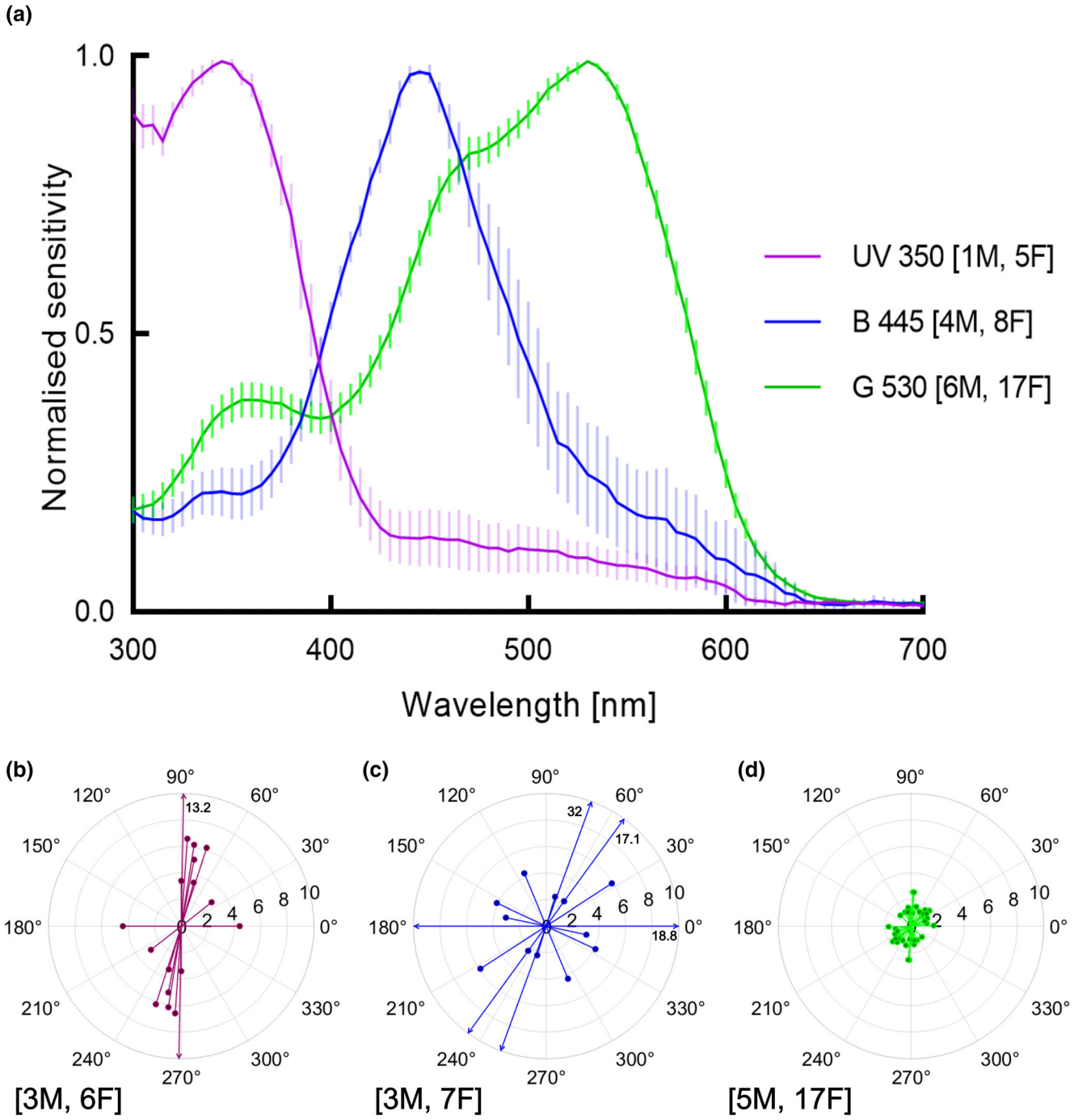

FIGURE 5 Spectral and polarization sensitivity of the photoreceptors measured via electrophysiological recordings. (a) Normalized spectral sensitivity of ultraviolet (UV), blue (B), and green (G) sensitive photoreceptors. Numbers indicate peak sensitivity wavelength (l_{max}) and [in brackets] the number of analysed cells separated by sex; lines and vertical bars indicate average and S.E.M. (b–d) Polarization sensitivity of all three photoreceptor types. Each photoreceptor measurement is represented by a pair of dots connected by a line in a circular vector plot. The direction of the line indicates φ_{max}, the angle of maximum sensitivity to linearly polarized light, while the length of the line represents the polarization sensitivity (PS), calculated as the ratio of maximum to minimum response amplitudes across different angles of polarization. Due to 180° symmetry, each measurement is shown in both directions. Where lines exceed the plotting radius, their endpoint is marked with an arrow and a numerical label indicating the PS value beyond the displayed scale.

Our findings suggest that vision is likely an important modality by which the meadow spittlebug *P. spumarius*, the primary vector of *X. fastidiosa* in all European outbreaks reported to date, locates host plants. Specifically, in addition to the substrate for trichromatic colour vision, *P. spumarius* exhibits both photoreceptor sensitivity to polarized light and polarotactic behaviour in controlled environments,

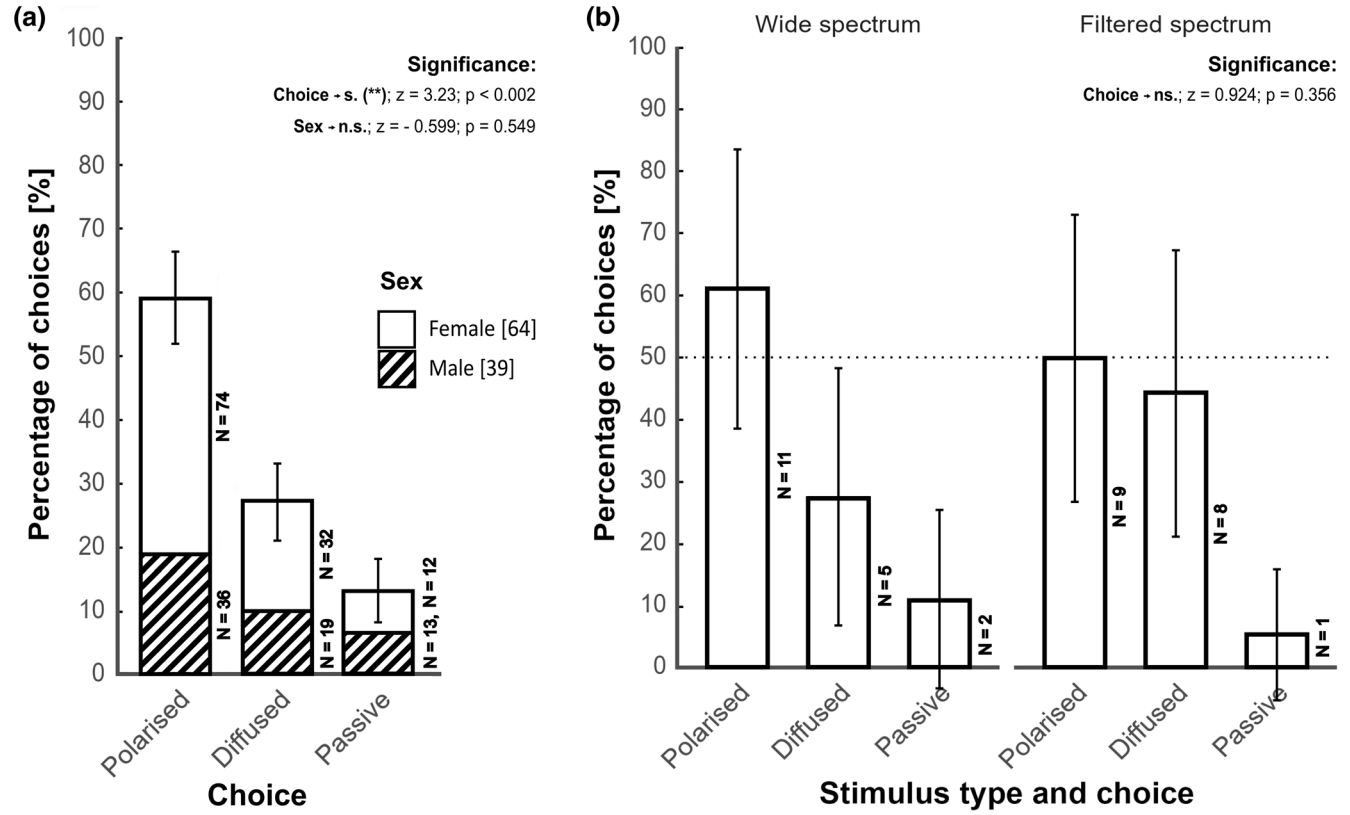

FIGURE 6 Plotted binomial GLMM for binary spittlebugs' responses to polarized and diffuse light stimuli (Passive excluded) with error bars representing 95% confidence intervals (CI). (a) Percentage of choices for polarized and diffuse stimuli in the first experiment, separated by sex: Females (white bars, $n = 118$ choices) and males (striped bars, $n = 68$ choices). A significant preference for polarized over diffuse was observed ($z = 3.23$, $p < .002^{**}$), with no significant difference between sexes ($z = -0.599$, $p = .599$). (b) GLMM analysis of the second experiment showing choices under wide-spectrum and yellow-restricted spectral conditions. The dotted line marks the random choice threshold at 50%. Across both light conditions, a total of 36 choices were analysed (pooled by sex). Statistical modelling showed no significant difference between the two spectral conditions ($z = 0.924$, $p = .356$), although the probability of choosing the polarized stimulus was higher under the broad-spectrum condition (0.688 ± 0.116 SE; 95% CI: 0.433–0.864) compared to the yellow-restricted condition (0.529 ± 0.121 SE; 95% CI: 0.303–0.745).

strongly suggesting that polarized light influences its decision-making processes. The visual system of *P. spumarius* has evolved to meet the ecological demands of its life cycle, transitioning from a sedentary nymphal stage to a highly mobile adult phase. Adults are extremely polyphagous and disperse across diverse landscape compartments, visiting a wide range of host plants (Casarin et al., 2023; Cornara et al., 2018), and such behavioural flexibility likely requires the integration of multiple sensory modalities. Vision may therefore play a role in detecting and evaluating host plants under variable environmental conditions, although its precise contribution to host location remains to be clarified (Prokopy & Owens, 1983).

Visual resolution is a critical prerequisite for perceiving target objects within the environment. Spatial resolution, or acuity, largely depends on morphological features of the eye, such as the interommatidial angles, the angles between individual facets (Land, 1997). According to our measurements, interommatidial angles ranged from 4° to 8°, consistent with previous findings for central ommatidia by Keskinen and Meyer-Rochow (2004). This range is typical of herbivorous insects that prioritize detecting larger, stationary objects as plants, over small, fast-moving targets, as in the case of predators (Land, 1997). Although *P. spumarius* lacks specialized high-acuity zones, its visual acuity is likely adequate for identifying larger objects, particularly against high-contrast backgrounds, an inference supported by studies on leafhoppers with comparable visual acuity (Tan et al., 2023; Zhang et al., 2018). This centrally improved resolution may still support forward-directed behaviours such as host detection or mating. With interommatidial angles narrowing to 4°–6°, *P. spumarius* may be able to detect targets at greater distances than aphids, which have a median angle of 7.9° and can detect a 2.6 cm object at around 19 cm (Döring & Spaethe, 2009). Extrapolating from these values, spittlebugs could theoretically detect the same target at approximately 30–35 cm, although this assumes similar neural processing capacities (Horridge, 1978; Land, 1997).

Consistent with predictions from opsin surveys in Hemiptera (Friedrich, 2023) and ERG studies in related *taxa* (Briscoe & Chittka, 2001; Kirchner et al., 2005), our electrophysiological recordings identified three photoreceptor types in *P. spumarius* with peaks in the ultraviolet (350 nm), blue (445 nm), and green (530 nm) ranges. This trichromatic arrangement provides the physiological basis for colour vision across the UV–green spectrum (Briscoe & Chittka, 2001;

van der Kooi et al., 2021). While such sensitivity may support host plant evaluation, its role is likely constrained by the strong similarity of leaf reflectance spectra under diffuse light, which largely reflects chlorophyll absorption outside of the 500–580 nm band (Prokopy & Owens, 1983). Spectral cues alone may therefore be insufficient for long-range host discrimination but could contribute at short range when combined with other visual, chemical, or tactile information during landing and probing (Anastasaki et al., 2021; Cornara et al., 2018, 2024; Germinara et al., 2017). Given *P. spumarius'* polyphagy, spectral sensitivity may serve primarily to detect plants within the environment, with final host acceptance depending on additional cues. The pronounced UV sensitivity of *P. spumarius* may also aid orientation and navigation in open habitats, as reported in other insects where UV enhances spatial awareness and directional control (Antignus et al., 1996, 2001; Lopez-Reyes et al., 2023).

Furthermore, our data suggest that the meadow spittlebugs are attracted by UV and blue horizontally polarized light, which might therefore play a crucial role in host finding. As the spittlebugs suffer from low spatial resolution, they likely use vision at short distances. Thus, when the spittlebug is standing upright or locomoting on the plant leaf, the cuticular reflection should always appear as horizontally polarized, irrespective of the leaf orientation. On the other hand, when viewed by the bug from a distance, numerous leaves, oriented at many different angles, create a display where randomly oriented polarized reflections cancel out and result in a diffuse, unpolarized appearance of a plant. We thus propose that horizontally polarized light from the waxy cuticles of leaves might represent an important environmental cue for *P. spumarius*. Electrophysiological measurements and anatomical evidence revealed a cellular substrate for object-directed, or ventral polarization vision mediated by the UV and blue-sensitive photoreceptors, whereas green-sensitive photoreceptors exhibited minimal or no sensitivity to polarization. This spectral specialization highlights the critical role of UV and blue wavelengths in detecting polarized light, a feature consistent with other insects where PS aids navigation and resource localization (Blake et al., 2019; Kelber, 1999; Kelber et al., 2001; Marshall & Cronin, 2011; Mathejczyk et al., 2023; Meglič et al., 2019; Wehner, 2001). However, we observed considerable variability in the maximum polarization responses of these receptors, which may stem from the invasive nature of intracellular recordings, the physiological state of the insect, metabolic differences between cells, or even adaptations of particular receptors for polarization vision. Overall, we hypothesize that linearly polarized light likely plays an important role in guiding *P. spumarius* towards vegetation (Blake et al., 2019; Kelber, 1999), which could augment other aspects of plant appearance and olfactory cues, especially in agroecosystems where visual cues are essential for navigating sparse or heterogeneous landscapes. This study of the meadow spittlebugs' optical properties and visual capabilities of individual photoreceptors in the retina establishes a solid foundation for future investigations into their mechanisms of host location and recognition.

Only a small proportion of individuals remained passive in the Y-maze, suggesting that *P. spumarius* is generally responsive to visual cues under experimental conditions. Orientation behaviour was elicited by visual information alone, supporting the suitability of the Y-maze for testing visually guided responses. In the ecological context of a mobile herbivore, such responsiveness is consistent with a functional role of visual cues, and particularly polarization, in host-finding. Our data, therefore, support the hypothesis that polarization contributes to decision-making. However, it remains unclear whether spittlebugs rely on polarization alone or in combination with spectral information when evaluating host plants, since the two cues often co-occur in natural environments and may interact in complex ways. Polarization can in some insects be perceived as a form of false colour, as shown in butterflies, while in others, such as bees, polarization is processed separately from colour (Kelber, 1999). Whether *P. spumarius* integrates polarization into its colour vision system or treats it as an independent channel of information is not yet known. Disentangling the relative contribution of colour and polarization will require further experiments under more naturalistic conditions.

No sex-specific differences were detected in any aspect of the visual system. Males and females showed comparable eye anatomy, spectral sensitivity, and responsiveness to polarized light, as well as similar behavioural responses in the Y-maze. Any sex-related variation in behaviour observed under natural conditions is therefore unlikely to be explained by differences in visual perception and may instead involve higher-level neural processes or interactions with other sensory modalities.

Overall, our results suggest that the visual capacities of *P. spumarius*, including potential for trichromatic colour vision and sensitivity to polarized light, could be exploited to reduce vector–plant contact. Visual interference methods such as reflective mulches, particle films, and colour-modified traps have already been shown to disrupt host location in other sap-feeding pests (Antignus et al., 2001; Döring, 2014; Summers et al., 2004; Tubajika et al., 2007), suggesting their potential for spittlebug management. Building on these approaches, knowledge of spittlebug visual sensitivities could support push–pull strategies, where crops or traps optimized to insect vision act as attractants while visual disruptors reduce host recognition. Breeding or selecting olive varieties with visual traits that are less attractive to the spittlebugs could be another viable strategy to limit the spread of the bacterium. Eventually, our findings highlighting the possible importance of vision in host finding by *P. spumarius*, that is, the main European vector of *X. fastidiosa*, pave the way for the development of new control strategies based on the interference with visual cues guiding the vector towards the host plant.

ACKNOWLEDGEMENTS

This research was funded by the European Union-NextGeneration EU, National Recovery and Resilience Plan (NRRP)—mission 4 component 2 investment 1.1—'Fund for the National Research Program and for Projects of National Interest (NRP)', CUP H53D23010620001, project KNOWS (Generating KNOWledge on insect-pathogen-agroecosystem interaction for a Sustainable *X. fastidiosa* control). It was also supported by the project SOS (Sviluppo di strategie di controllo sostenibili di *P. spumarius* ed

interferenza con la trasmissione di *X. fastidiosa*), grant agreement D23C22001020001, funded by the Italian Ministry of Agriculture, Food Sovereignty and Forestry (MASAF). This study was financially supported by the AFOSR/EOARD (grant no. FA8655-23-1-7049 to G.B.) and by the Slovenian Research Agency (grant no. P3-0333 to G.B.). This research used resources of the Advanced Light Source, a U.S. DOE Office of Science User Facility under contract no. DE-AC02-05CH11231. We thank Marko Ilić and Uroš Cerkvenik from the University of Ljubljana for their valuable support in data analysis and help in establishing the pseudopupil tracking methodology.

CONFLICT OF INTEREST STATEMENT

The authors have no relevant financial or non-financial interests to disclose.

DATA AVAILABILITY STATEMENT

Raw datasets and supplemental info are available from the corresponding author upon request.

ORCID

Daniele Cornara https://orcid.org/0000-0001-8258-2291

REFERENCES

Anastasaki, E., Psoma, A., Partsinevelos, G., Papachristos, D., & Milonas, P. (2021). Electrophysiological responses of *Philaenus spumarius* and *Neophilaenus campestris* females to plant volatiles. *Phytochemistry*, *189*, 112848. https://doi.org/10.1016/j.phytochem.2021.112848

Antignus, Y. (2000). Manipulation of wavelength-dependent behaviour of insects: An IPM tool to impede insects and restrict epidemics of insect-borne viruses. *Virus Research*, *71*, 213–220. https://doi.org/10.1016/S0168-1702(00)00199-4

Antignus, Y., Mor, N., Ben Joseph, R., Lapidot, M., & Cohen, S. (1996). Ultraviolet-absorbing plastic sheets protect crops from insect pests and from virus diseases vectored by insects. *Environmental Entomology*, *25*, 919–924. https://doi.org/10.1093/ee/25.5.919

Antignus, Y., Nestel, D., Cohen, S., & Lapidot, M. (2001). Ultraviolet-deficient greenhouse environment affects whitefly attraction and flight behavior. *Environmental Entomology*, *30*, 394–399. https://doi.org/10.1603/0046-225X-30.2.394

Arikawa, K., Inokuma, K., & Eguchi, E. (1987). Pentachromatic visual system in a butterfly. *Naturwissenschaften*, *74*(6), 297–298. https://doi.org/10.1007/BF00366422

Athanasiadou, M., Schulz, M., & Meyhöfer, R. (2024). The effect of blue and UV light-emitted diodes (LEDs) on the disturbance of the whitefly natural enemies *Macrolophus pygmaeus* and *Encarsia formosa*. *Biological Control*, *199*, 105663. https://doi.org/10.1016/j.biocontrol.2024.105663

Avosani, S., Nieri, R., Mazzoni, V., Anfora, G., Hamouche, Z., Zippari, C., Vitale, M. L., Verrastro, V., Tarasco, E., D'Isita, I., Germinara, S., Döring, T. F., Belušič, G., Fereres, A., Thompson, V., & Cornara, D. (2024). Intruding into a conversation: How behavioral manipulation could support management of *Xylella fastidiosa* and its insect vectors. *Journal of Pest Science*, *97*, 17–33. https://doi.org/10.1007/s10340-023-01631-7

Belušič, G., de Hoop, S. B., Bencúrová, E., Lazar, D., Spaethe, J., & van der Kooi, C. J. (2025). Remarkable red colour vision in two Mediterranean beetle pollinators. *Journal of Experimental Biology*, *228*(12), jeb250181. https://doi.org/10.1242/jeb.250181

Belušič, G., Ilić, M., Meglič, A., & Pirih, P. (2016). A fast multispectral light synthesiser based on LEDs and a diffraction grating. *Scientific Reports*, *6*, 32012. https://doi.org/10.1038/srep32012

Belušič, G., Šporar, K., & Meglič, A. (2017). Extreme polarisation sensitivity in the retina of the corn borer moth *Ostrinia*. *Journal of Experimental Biology*, *220*(11), 2047–2056. https://doi.org/10.1242/jeb.153718

Ben-Yakir, D. (Ed.). (2020). *Optical manipulation of arthropod pests and beneficials*. CABI. https://doi.org/10.1079/9781786394705.0001

Ben-Yakir, D., Antignus, Y., Offir, Y., & Shahak, Y. (2013). Optical manipulations: An advanced approach for reducing sucking insect pests. In A. R. Horowitz & I. Ishaaya (Eds.), *Advanced technologies for managing insect pests* (pp. 249–267). Springer. https://doi.org/10.1007/978-94-007-4497-4_12

Bernard, G. D., & Remington, C. L. (1991). Color vision in Lycaena butterflies: Spectral tuning of receptor arrays in relation to behavioral ecology. *Proceedings of the National Academy of Sciences of the United States of America*, *88*(7), 2783–2787. https://doi.org/10.1073/pnas.88.7.2783

Blake, A. J., Go, M. C., Hahn, G. S., Grey, H., Couture, S., & Gries, G. (2019). Polarization of foliar reflectance: Novel host plant cue for insect herbivores. *Proceedings of the Royal Society B*, *286*, 20192198. https://doi.org/10.1098/rspb.2019.2198

Briscoe, A. D. (2000). Six opsins from the butterfly *Papilio glaucus*: Molecular phylogenetic evidence for paralogous origins of red-sensitive visual pigments in insects. *Journal of Molecular Evolution*, *51*(2), 110–121. https://doi.org/10.1007/s002390010071

Briscoe, A. D., Bernard, G. D., Szeto, A. S., Nagy, L. M., & White, R. H. (2003). Not all butterfly eyes are created equal: Rhodopsin absorption spectra, molecular identification, and localization of ultraviolet-, blue-, and green-sensitive rhodopsin-encoding mRNAs in the retina of *Vanessa cardui*. *Journal of Comparative Neurology*, *458*(4), 334–349. https://doi.org/10.1002/cne.10582

Briscoe, A. D., & Chittka, L. (2001). The evolution of color vision in insects. *Annual Review of Entomology*, *46*, 471–510. https://doi.org/10.1146/annurev.ento.46.1.471

Brooks, M. E., Kristensen, K., Van Benthem, K. J., Magnusson, A., Berg, C. W., Nielsen, A., Skaug, H. J., Mächler, M., & Bolker, B. M. (2017). glmmTMB balances speed and flexibility among packages for zero-inflated generalized linear mixed modeling. *The R Journal*, *9*(2), 378–400. https://doi.org/10.32614/RJ-2017-066

Bruckmoser, P. (1968). Die spektrale Empfindlichkeit einzelner Sehzellen des Rückenschwimmers Notonecta glauca L. (Heteroptera). *Zeitschrift für Vergleichende Physiologie*, *59*, 187–204. https://doi.org/10.1007/BF00339349

Cardona, A., Saalfeld, S., Schindelin, J., Arganda-Carreras, I., Preibisch, S., Longair, M., & Douglas, R. J. (2012). TrakEM2 software for neural circuit reconstruction. *PLoS One*, *7*, e38011. https://doi.org/10.1371/journal.pone.0038011

Casarin, N., Hasbroucq, S., Carestia, G., Glibert, A., Bragard, C., & Grégoire, J. C. (2023). Investigating dispersal abilities of Aphrophoridae in European temperate regions to assess the threat of potential *Xylella fastidiosa*-based pathosystems. *Journal of Pest Science*, *96*(2), 471–488. https://doi.org/10.1007/s10340-022-01562-9

Cascone, P., Quarto, R., Iodice, L., Cencetti, G., Formisano, G., Spiezia, G., & Guerrieri, E. (2022). Behavioural response of the main vector of *Xylella fastidiosa* towards olive VOCs. *Entomologia Generalis*, *42*, 35–44. https://doi.org/10.1127/entomologia/2021/1218

Chen, P.-J., Awata, H., Matsushita, A., Yang, E.-C., & Arikawa, K. (2016). Extreme spectral richness in the eye of the common bluebottle butterfly, Graphium sarpedon. *Frontiers in Ecology and Evolution*, *4*, 18.

Chittka, L. (1997). Bee color vision is optimal for coding flower color, but flower colors are not optimal for being coded—why? *Israel Journal of Plant Sciences*, *45*, 115–127. https://doi.org/10.1080/07929978.1997.10676678

Chittka, L., & Menzel, R. (1992). The evolutionary adaptation of flower colours and the insect pollinators' colour vision. *Journal of Comparative Physiology A*, *171*, 171–181. https://doi.org/10.1007/BF00188925

Clark, E. G., Cornara, D., Brodersen, C. R., McElrone, A. J., Parkinson, D. Y., & Almeida, R. P. (2023). Anatomy of an agricultural antagonist: Feeding complex structure and function of three xylem sap-feeding insects illuminated with synchrotron-based 3D imaging. *Journal of Morphology*, *284*, e21639. https://doi.org/10.1002/jmor.21639

Coombe, P. E. (1981). Wavelength specific behaviour of the whitefly *Trialewodes vaporariorum* (Homoptera: Aleyrodidae). *Journal of Comparative Physiology*, *144*, 83–90. https://doi.org/10.1007/BF00612801

Cornara, D., Bojanini, I., Fereres, A., & Almeida, R. P. P. (2024). Definitive elucidation of the inoculation mechanism of *Xylella fastidiosa* by sharpshooter leafhoppers. *Entomologia Generalis*, *44*(1), 121–131. https://doi.org/10.1127/entomologia/2023/2126

Cornara, D., Bosco, D., & Fereres, A. (2018). *Philaenus spumarius*: When an old acquaintance becomes a new threat to European agriculture. *Journal of Pest Science*, *91*, 957–972. https://doi.org/10.1007/s10340-018-0966-0

Cornara, D., Saponari, M., Zeilinger, A. R., de Stradis, A., Boscia, D., Loconsole, G., & Porcelli, F. (2017). Spittlebugs as vectors of *Xylella fastidiosa* in olive orchards in Italy. *Journal of Pest Science*, *90*, 521–530. https://doi.org/10.1007/s10340-016-0793-0

Cruaud, A., Gonzalez, A. A., Godefroid, M., Nidelet, S., Streito, J. C., Thuillier, J. M., Rossi, J. P., Santoni, S., & Rasplus, J. Y. (2018). Using insects to detect, monitor and predict the distribution of *Xylella fastidiosa*: A case study in Corsica. *Scientific Reports*, *8*, 15628. https://doi.org/10.1038/s41598-018-33957-z

Daugherty, M. P., O'Neill, S., Byrne, F., & Zeilinger, A. (2015). Is vector control sufficient to limit pathogen spread in vineyards? *Environmental Entomology*, *44*, 789–797. https://doi.org/10.1093/ee/nvv046

Döring, T. F. (2014). How aphids find their host plants and how they don't. *Annals of Applied Biology*, *165*, 3–26. https://doi.org/10.1111/aab.12142

Döring, T. F., & Spaethe, J. (2009). Measurements of eye size and acuity in aphids (Hemiptera: Aphididae). *Entomologia Generalis*, *32*, 77–84. https://doi.org/10.1127/entom.gen/32/2009/77

Foster, J. J., Temple, S. E., How, M. J., Daly, I. M., Sharkey, C. R., Wilby, D., & Roberts, N. W. (2018). Polarisation vision: Overcoming challenges of working with a property of light we barely see. *The Science of Nature*, *105*(3), 27. https://doi.org/10.1007/s00114-018-1551-3

Franceschini, N., & Kirschfeld, K. (1971). Les phénomènes de pseudopupille dans l'œil composé de *Drosophila*. *Kybernetik*, *9*, 159–182. https://doi.org/10.1007/BF02215177

Friedrich, M. (2023). Parallel losses of blue opsin correlate with compensatory neofunctionalization of UV-opsin gene duplicates in aphids and planthoppers. *Insects*, *14*, 774. https://doi.org/10.3390/insects14090774

Germinara, G. S., Ganassi, S., Pistillo, M. O., Di Domenico, C., De Cristofaro, A., & Di Palma, A. M. (2017). Antennal olfactory responses of adult meadow spittlebug, *Philaenus spumarius*, to volatile organic compounds (VOCs). *PLoS One*, *12*, e0190454. https://doi.org/10.1371/journal.pone.0190454

Gogala, M. (1967). Die spektrale Empfindlichkeit der Doppelaugen von *Ascalaphus macaronius* Scop. (Neuroptera, Ascalaphidae). *Zeitschrift für Vergleichende Physiologie*, *57*(3), 232–243. https://doi.org/10.1007/BF00302998

Grant, L., Daughtry, C. S. T., & Vanderbilt, V. C. (1993). Polarized and specular reflectance variation with leaf surface features. *Physiologia Plantarum*, *88*(1), 1–9. https://doi.org/10.1111/j.1399-3054.1993.tb01753.x

Gürsoy, D., De Carlo, F., Xiao, X., & Jacobsen, C. (2014). TomoPy: A framework for the analysis of synchrotron tomographic data. *Journal of Synchrotron Radiation*, *21*, 1188–1193. https://doi.org/10.1107/S1600577514013939

Hardie, R. C. (1986). The photoreceptor array of the dipteran retina. *Trends in Neurosciences*, *9*, 419–423. https://doi.org/10.1016/0166-2236(86)90136.10.1016/0166-2236(86)90136-0

Hariyama, T., Tsukahara, Y., & Meyer-Rochow, V. B. (1993). Spectral responses, including a UV-sensitive cell type, in the eye of the isopod *Ligia exotica*. *Naturwissenschaften*, *80*(5), 233–235. https://doi.org/10.1007/BF01175741

Hartig, F. (2016). DHARMa: Residual diagnostics for hierarchical (multi-level/mixed) regression models (R package version 0.1.0) [Computer software]. *Comprehensive R Archive Network (CRAN)*. https://cran.r-project.org/package=DHARMa

Heinloth, T., Uhlhorn, J., & Wernet, M. F. (2018). Insect responses to linearly polarized reflections: Orphan behaviors without neural circuits. *Frontiers in Cellular Neuroscience*, *12*, 50. https://doi.org/10.3389/fncel.2018.00050

Heras, F. J., & Laughlin, S. B. (2017). Optimizing the use of a sensor resource for opponent polarization coding. *PeerJ*, *5*, e2772. https://doi.org/10.7287/peerj.preprints.2192v1

Homberg, U. (2015). Sky compass orientation in desert locusts-evidence from field and laboratory studies. *Frontiers in Behavioral Neuroscience*, *9*, 346. https://doi.org/10.3389/fnbeh.2015.00346

Horridge, G. A. (1978). The separation of visual axes in apposition compound eyes. *Philosophical Transactions of the Royal Society of London B: Biological Sciences*, *285*, 1–59. https://doi.org/10.1098/rstb.1978.0093

Ichikawa, T., & Tateda, H. (1982). Distribution of color receptors in the larval eyes of four species of Lepidoptera. *Journal of Comparative Physiology*, *149*(3), 317–324. https://doi.org/10.1007/BF00619147

Kelber, A. (1999). Why 'false' colours are seen by butterflies. *Nature*, *402*, 251. https://doi.org/10.1038/46204

Kelber, A., Thunell, C., & Arikawa, K. (2001). Polarisation-dependent colour vision in *Papilio* butterflies. *Journal of Experimental Biology*, *204*, 2469–2480. https://doi.org/10.1242/jeb.204.14.2469

Keskinen, E., & Meyer-Rochow, V. B. (2004). Post-embryonic photoreceptor development and dark/light adaptation in the spittle bug *Philaenus spumarius* (L.) (Homoptera, Cercopidae). *Arthropod Structure & Development*, *33*, 405–417. https://doi.org/10.1016/j.asd.2004.05.010

Kinoshita, M., Sato, M., & Arikawa, K. (1997). Spectral receptors of nymphalid butterflies. *Naturwissenschaften*, *84*(5), 199–201. https://doi.org/10.1007/s001140050377

Kirchner, S. M., Döring, T. F., & Saucke, H. (2005). Evidence for trichromacy in the green peach aphid, *Myzus persicae* (Sulz.) (Hemiptera: Aphididae). *Journal of Insect Physiology*, *51*, 1255–1260. https://doi.org/10.1016/j.jinsphys.2005.07.002

Kirwan, J. D., Graf, J., Smolka, J., Mayer, G., Henze, M. J., & Nilsson, D. E. (2018). Low-resolution vision in a velvet worm (Onychophora). *Journal of Experimental Biology*, *221*, jeb175802. https://doi.org/10.1242/jeb.175802

Labhart, T., & Meyer, E. P. (1999). Detectors for polarized skylight in insects: A survey of ommatidial specializations in the dorsal rim area of the compound eye. *Microscopy Research and Technique*, *47*, 368–379. https://doi.org/10.1002/(sici)1097-0029(19991215)47:6<368::aid-jemt2>3.0.co;2-q

Labhart, T., & Wehner, R. (2006). Polarization vision. In E. J. Warrant & D. E. Nilsson (Eds.), *Invertebrate vision* (pp. 291–348). Cambridge University Press.

Land, M. F. (1989). Variations in the structure and design of compound eyes. In D. G. Stavenga & R. C. Hardie (Eds.), *Facets of vision* (pp. 90–111). Springer. https://doi.org/10.1007/978-3-642-74082-4_5

Land, M. F. (1997). Visual acuity in insects. *Annual Review of Entomology*, *42*, 147–177. https://doi.org/10.1146/annurev.ento.42.1.147

Land, M. F., & Fernald, R. D. (1992). The evolution of eyes. *Annual Review of Neuroscience*, *15*, 1–29. https://doi.org/10.1146/annurev.ne.15.030192.000245

Land, M. F., & Nilsson, D. E. (2012). *Animal eyes* (2nd ed.). Oxford University Press. https://doi.org/10.1093/acprof:oso/9780199581139.001.0001

Lopez-Reyes, K., Lankheet, M. J., van Tol, R. W., Butler, R. C., Teulon, D. A., & Armstrong, K. F. (2023). Tracking the flight and landing behaviour of western flower thrips in response to single and two-colour cues. *Scientific Reports*, *13*, 14178. https://doi.org/10.1038/s41598-023-37400-w

Marshall, J., & Cronin, T. W. (2011). Polarisation vision. *Current Biology*, *21*, R101–R105. https://doi.org/10.1016/j.cub.2010.12.012

Mathejczyk, T. F., Babo, É. J., Schönlein, E., Grinda, N. V., Greiner, A., Okrožnik, N., & Wernet, M. F. (2023). Behavioral responses of free-flying *Drosophila melanogaster* to shiny, reflecting surfaces. *Journal of Comparative Physiology A*, *209*, 929–941. https://doi.org/10.1007/s00359-023-01676-0

Maxwell, D. J., Partridge, J. C., Roberts, N. W., Boonham, N., & Foster, G. D. (2016). The effects of plant virus infection on polarization reflection from leaves. *PLoS One*, *11*(4), e0152836. https://doi.org/10.1371/journal.pone.0152836

Meglič, A., Ilić, M., Pirih, P., Škorjanc, A., Wehling, M. F., Kreft, M., & Belušič, G. (2019). Horsefly object-directed polarotaxis is mediated by a stochastically distributed ommatidial subtype in the ventral retina. *Proceedings of the National Academy of Sciences of the United States of America*, *116*, 21843–21853. https://doi.org/10.1073/pnas.1910807116

Moralejo, E., Borràs, D., Gomila, M., Montesinos, M., Adrover, F., Juan, A., Nieto, A., Olmo, D., Seguí, G., & Landa, B. B. (2019). Insights into the epidemiology of Pierce's disease in vineyards of Mallorca, Spain. *Plant Pathology*, *68*, 1458–1471. https://doi.org/10.1111/ppa.13076

Nilsson, D. E., & Warrant, E. J. (1999). Visual discrimination: Seeing the third quality of light. *Current Biology*, *9*, R535–R537. https://doi.org/10.1016/s0960-9822(99)80330-3

Ogawa, Y., Kinoshita, M., Stavenga, D. G., & Arikawa, K. (2013). Sex-specific retinal pigmentation results in sexually dimorphic long-wavelength-sensitive photoreceptors in the eastern pale clouded yellow butterfly, *Colias erate*. *Journal of Experimental Biology*, *216*(10), 1916–1923. https://doi.org/10.1242/jeb.083485

Pirih, P., Meglič, A., Stavenga, D., Arikawa, K., & Belušič, G. (2020). The red admiral butterfly's living light sensors and signals. *Faraday Discussions*, *223*, 81–97. https://doi.org/10.1039/D0FD00075B

Prokopy, R. J., & Owens, E. D. (1983). Visual detection of plants by herbivorous insects. *Annual Review of Entomology*, *28*, 337–359. https://doi.org/10.1146/annurev.en.28.010183.002005

Purcell, A. H., & Finlay, A. H. (1979). Evidence for noncirculative transmission of Pierce's disease bacterium by sharpshooter leafhoppers. *Phytopathology*, *69*(4), 393–395. https://www.apsnet.org/publications/phytopathology/backissues/Documents/1979Articles/Phyto69n04_393.pdf

R Core Team. (2020). *R: A language and environment for statistical computing*. R Foundation for Statistical Computing. https://www.r-project.org/

Ranieri, E., Ruschioni, S., Riolo, P., Isidoro, N., & Romani, R. (2016). Fine structure of antennal sensilla of the spittlebug *Philaenus spumarius* L. (Insecta: Hemiptera: Aphrophoridae). I. Chemoreceptors and thermo-/hygroreceptors. *Arthropod Structure & Development*, *45*, 432–449. https://doi.org/10.1016/j.asd.2016.09.005

Rayer, B., Naynert, M., & Stieve, H. (1990). New trends in photobiology: Phototransduction: Different mechanisms in vertebrates and invertebrates. *Journal of Photochemistry and Photobiology, B: Biology*, *7*, 107–148. https://doi.org/10.1016/1011-1344(90)85151-L

Reeves, J. L. (2011). Vision should not be overlooked as an important sensory modality for finding host plants. *Environmental Entomology*, *40*(4), 855–863. https://doi.org/10.1603/EN10212

Roberts, N. W., Porter, M. L., & Cronin, T. W. (2011). The molecular basis of mechanisms underlying polarization vision. *Philosophical Transactions of the Royal Society of London. Series B, Biological Sciences*, *366*, 627–637. https://doi.org/10.1098/rstb.2010.0206

Rodrigues, I., Benhadi-Marín, J., Rodrigues, N., Baptista, P., & Pereira, J. A. (2022). Olfactory responses to volatile organic compounds and movement parameters of *Philaenus spumarius* and *Cicadella viridis*. *Journal of Applied Entomology*, *146*, 486–497. https://doi.org/10.1111/jen.12992

Rossel, S. (1980). Foveal fixation and tracking in the praying mantis. *Journal of Comparative Physiology*, *139*, 307–331. https://doi.org/10.1007/BF00610462

Santer, R. D., & Allen, W. L. (2024). Optimising the colour of traps requires an insect's eye view. *Pest Management Science*, *80*(3), 931–934. https://doi.org/10.1002/ps.7790

Schindelin, J., Arganda-Carreras, I., Frise, E., Kaynig, V., Longair, M., Pietzsch, T., & Cardona, A. (2012). Fiji: An open-source platform for biological-image analysis. *Nature Methods*, *9*, 676–682. https://doi.org/10.1038/nmeth.2019

Seki, T., & Vogt, K. (1998). Evolutionary aspects of the diversity of visual pigment chromophores in the class Insecta. *Comparative Biochemistry and Physiology Part B: Biochemistry and Molecular Biology*, *119*(1), 53–64. https://doi.org/10.1016/S0305-0491(97)00322-2

Sherk, T. E. (1977). Development of the compound eyes of dragonflies (Odonata). I. Larval compound eyes. *Journal of Experimental Zoology*, *201*, 391–416. https://doi.org/10.1002/jez.1402010307

Stavenga, D. G. (1975). Optical qualities of the fly eye: An approach from the side of geometrical, physical and waveguide optics. In A. W. Snyder & R. Menzel (Eds.), *Photoreceptor optics* (pp. 83–111). Springer. https://doi.org/10.1007/978-3-642-80934-7_7

Summers, C. G., Mitchell, J. P., & Stapleton, J. J. (2004). Management of aphid-borne viruses and *Bemisia argentifolii* (Homoptera: Aleyrodidae) in zucchini squash by using UV reflective plastic and wheat straw mulches. *Environmental Entomology*, *33*, 1447–1457. https://doi.org/10.1603/0046-225X-33.5.1447

Tan, C., Cai, X., Luo, Z., Li, Z., Xiu, C., Chen, Z., & Bian, L. (2023). Visual acuity of *Empoasca onukii* (Hemiptera, Cicadellidae). *Insects*, *14*, 370. https://doi.org/10.3390/insects14040370

Thompson, V., Harkin, C., & Stewart, A. J. (2023). The most polyphagous insect herbivore? Host plant associations of the meadow spittlebug, *Philaenus spumarius* (L.). *PLoS One*, *18*, e0291734. https://doi.org/10.1371/journal.pone.0291734

Tubajika, K. M., Civerolo, E. L., Puterka, G. J., Hashim, J. M., & Luvisi, D. A. (2007). The effects of kaolin, harpin, and imidacloprid on the development of Pierce's disease in grape. *Crop Protection*, *26*(2), 92–99. https://doi.org/10.1016/j.cropro.2006.04.006

Van Der Kooi, C. J., Stavenga, D. G., Arikawa, K., Belušič, G., & Kelber, A. (2021). Evolution of insect color vision: From spectral sensitivity to visual ecology. *Annual Review of Entomology*, *66*, 435–461. https://doi.org/10.1146/annurev-ento-061720-071644

Wehner, R. (1976). Polarized-light navigation by insects. *Scientific American*, *235*, 106–115. https://doi.org/10.1038/scientificamerican0776-106

Wehner, R. (2001). Polarization vision—A uniform sensory capacity? *Journal of Experimental Biology*, *204*, 2589–2596. https://doi.org/10.1242/jeb.204.14.2589

Wehner, R. (2014). Polarization vision: A discovery story. In G. Horváth (Ed.), *Polarized light and polarization vision in animal sciences* (pp. 3–19). Springer. https://doi.org/10.1007/978-3-642-54718-8_1

White, R. H., Stevenson, R. D., Bennett, R. R., Cutler, D. E., & Haber, W. A. (1994). Wavelength discrimination and the role of ultraviolet vision in the feeding behavior of hawkmoths. *Biotropica*, *26*, 427–435. https://doi.org/10.2307/2389237

Wood, H. M., & Parkinson, D. Y. (2019). Comparative morphology of cheliceral muscles using high-resolution X-ray microcomputed-tomography in palpimanoid spiders (Araneae, Palpimanoidea). *Journal of Morphology*, *280*, 232–243. https://doi.org/10.1002/jmor.20939

Zhang, X., Pengsakul, T., Tukayo, M., Yu, L., Fang, W., & Luo, D. (2018). Host-location behavior of the tea green leafhopper *Empoasca vitis* Göthe (Hemiptera: Cicadellidae): Olfactory and visual effects on their orientation. *Bulletin of Entomological Research*, *108*, 423–433. https://doi.org/10.1017/S0007485317000931

SUPPORTING INFORMATION

Additional supporting information can be found online in the Supporting Information section at the end of this article.

How to cite this article: Lazar, D., Clark, E., Meglič, A., Cornara, D., & Belušič, G. (2026). Polarization vision and the physiological basis for trichromatic vision in *Philaenus spumarius*: Understanding host-seeking behaviour in insect vectors for *Xylella fastidiosa* control. *Annals of Applied Biology*, *188*(2), 503–519. https://doi.org/10.1111/aab.70065